smaller dimensions relative to larger, less stable tunnels or sheet structures. Further examination of marine and terrestrial todorokite by high-resolution imaging and concurrent chemical microanalysis is necessary to determine if a relationship exists between chemical composition and tunnel dimensions.

MALCOLM D. SIEGEL
Organization 9413,
Sandia National Laboratories,
Albuquerque, New Mexico 87185
SHIRLEY TURNER
Department of Geology,
Arizona State University, Tempe 85287

References and Notes

1. R. G. Burns and V. M. Burns, in *Marine Manganese Deposits*, G. P. Glasby, Ed. (Elsevier, Amsterdam, 1977), pp. 185–248; *Scanning Electron Microsc.* **1**, 245 (1978).
2. J. A. Straczek, A. Horen, M. Ross, C. M. Warshaw, *Am. Mineral.* **45**, 1174 (1960); F. T. Manheim, in *Symposium on Marine Chemistry*, D. R. Schink and J. T. Corliss, Eds. (Occasional Publication, University of Rhode Island, 1965), vol. 3, pp. 217–276.
3. W. Buser and A. Grutter, *Schweiz. Mineral. Petrog. Mitt.* **36**, 49 (1956); R. Giovanoli, W. Feitknecht, F. Fischer, *Helv. Chim. Acta* **54**, 1112 (1971).
4. F. V. Chukhrov *et al.*, *Nature (London)* **278**, 631 (1979); *Int. Geol. Rev.* **22**, 75 (1980).
5. M. D. Siegel, *Geol. Soc. Am. Abstr. Programs* **11**, 516 (1979).
6. _____, thesis, Harvard University (1981).
7. S. Turner, M. D. Siegel, P. R. Buseck, *Eos* **62**, 306 (1981); *Nature (London)* **296**, 841 (1982).
8. S. Turner and P. R. Buseck, *Science* **212**, 1024 (1981).
9. M. Karas, thesis, Scripps Institution of Oceanography (1978).
10. Quantitative point analyses for 17 elements were obtained at the Department of Geological Sciences, Harvard University, with an automated Applied Research Laboratories EMX-SM electron microprobe and the correction method outlined by A. Bence and A. Albee [*J. Geol.* **76**, 322 (1968)] and A. Albee and L. Ray [*Anal. Chem.* **42**, 1408 (1970)].
11. Debye-Scherrer x-ray diffraction patterns were obtained with manganese-filtered Fe Kα radiation. The least-squares refinement of the unit cell parameters was calculated with the use of LCLSQ, a program written by C. W. Burnham, Department of Geological Sciences, Harvard University.
12. Samples of nodule cores were ground to a fine powder under water, suspended in water, and applied to a carbon film supported by a 200-mesh grid. Electron diffraction patterns and structural images of this material were obtained in a slightly modified JEOL JEM 100B microscope [D. R. Veblen and P. R. Buseck, *Am. Mineral.* **64**, 687 (1979)].
13. A. Usui, thesis, University of Tokyo (1979).
14. P. Halbach and M. Ozkara, in *La genèse des nodules manganese* (No. 289, Collection Internationale du Centre National de la Recherche Scientifique, Paris, 1979), pp. 77–88.
15. A. Bystrom and A. M. Bystrom, *Acta Crystallogr.* **3**, 146 (1950).
16. We are grateful to K. Jones, M. Carpenter, and E. Seeling for their assistance with the electron microscopy. Samples were provided from the MANOP nodule collection by T. Walsh. We thank H. D. Holland, P. Buseck, and R. Burns for their guidance and support of this research. This work was supported by grants EAR79-26375 and EAR79-04364 from the Earth Sciences Division of the National Science Foundation (NSF) and grant 832550CE from the NSF International Decade of Oceanographic Exploration Manganese Nodule Program.

5 May 1982; revised 17 August 1982

Recombination During Gene Transfer into Mouse Cells Can Restore the Function of Deleted Genes

Abstract. *Two plasmids containing nonoverlapping deletions of the herpes simplex virus thymidine kinase gene were introduced into thymidine kinase–deficient mouse L cells by DNA-mediated gene transfer. Thymidine kinase–producing transformants were generated by a mixture of the two plasmids at a frequency significantly greater than that generated by either plasmid alone. Southern blot analyses demonstrated that functional thymidine kinase genes were generated by homologous recombination between the two deletion mutants.*

In prokaryotic systems, the integration of exogenously added DNA into the genome of recipient cells occurs primarily through homologous recombination (*1*). In eukaryotic cells, integration has been studied most extensively in yeast, where it occurs both at sites of homology and at sites not linked to the cellular homolog (*2–4*). In some cases, genes are integrated by double crossover events to replace the cellular gene (*4*).

Previous experiments in which DNA was introduced into mammalian cells and embryos demonstrated that exogenous DNA integrated at many sites in the genome (*5–9*), so that the integrations appeared random. An apparent absence of homologous recombination might be explained by several hypotheses.

1) In experiments in which calcium phosphate was coprecipitated with DNA, large complexes of the input DNA (termed pekelasomes or transgenomes) were found in the recipient cell (*5, 8, 9*). Since most transfer experiments include whole cell DNA either as a carrier or donor, integration at sites homologous to the DNA in the transgenome could occur at many sites and appear random.

2) In many systems, including the widely used thymidine kinase (TK) gene of herpes simplex virus (HSV), no DNA in the recipient cell was homologous to the selected exogenous gene. Therefore, even if homologous recombination were possible, it would not have been detected.

3) The mammalian genome is 750 times larger than the *Escherichia coli* genome (*10*), so that even if a homologous gene were the most common integration site, the sum of integration events at sites of partial or no homology might be greater.

Sister chromatid exchange, meiotic recombination, immunoglobulin gene rearrangements (*11–13*), and the demonstration of recombination between SV40 molecules (*14*) suggest that the machinery necessary for homologous recombination is present in mammalian cells. Recombination between independent molecules has been detected during gene transfer (*15*), but previous experiments did not distinguish between random and homologous recombination. We now describe experiments designed to determine whether homologous recombination could occur between two plasmids containing nonoverlapping deletions in the TK gene during DNA-mediated gene transfer.

Two deletion mutants of the HSV TK gene were cloned into the plasmid pBR322 (see Fig. 1C). The functionally wild-type plasmid, pTK−109 (referred to herein as −109), contains a 1.7 kilobase pair (kbp) fragment of HSV DNA that includes an intact structural TK gene and its 5′ control region. One deletion mutant, pTK+25 (herein referred to as +25), has a 5′ deletion extending to 25 base pairs (bp) beyond the cap site. It has an intact structural gene but lacks all important 5′ control sites (*16*). The second deletion mutant, pTKΔ23 (referred to as Δ23) was prepared by digestion of −109 with the restriction endonuclease Kpn I, which cuts the plasmid once within the TK structural gene (Fig. 1C). The DNA was digested with S1 nuclease to remove the 4-base single-stranded ends and then ligated. This procedure generated a small deletion within the TK structural gene and left the 5′ control region intact (Fig. 1C). Both +25 and Δ23 are deletion mutants of the functional parental gene, −109, with +25 missing the 5′ sequences that regulate transcription and Δ23 having a small deletion within the TK structural gene.

Each of the plasmids alone and a mixture of +25 and Δ23 were precipitated onto cells of the TK-deficient mouse L cell line, Ltk$^-$, in the absence of carrier DNA. The number of thymidine kinase–producing (TK$^+$) colonies generated by each plasmid or mixture is given in Table 1. The 5′ deletion mutant +25 generated colonies at a frequency 90-fold less than that of the wild type, and Δ23 generated no colonies in any experiments. The mixture of +25 and Δ23 generated colonies at a frequency ninefold lower than that of the wild-type control and tenfold higher than that of +25 alone.

These results suggested that the +25 and Δ23 genes interacted with each other to generate functional TK molecules. Two possibilities exist: +25 and Δ23 may have formed concatamers whereby the Δ23 promoter at low frequency could read through the Δ23 and +25 genes and thereby generate functional TK messenger RNA (mRNA). Alternatively, recombination may have generated a functional TK gene. Southern blot analyses (*17*) were performed to distinguish between these possibilities. If TK^+ cell lines were formed by concatamerization of plasmids, then only bands derived from +25 and Δ23 plasmids should be seen. If recombination had occurred, then not only the bands generated by the +25 and Δ23 genes, but also bands generated by a recombinant functional gene would be present; the latter would be equivalent in size to bands generated from the parental gene −109. Also, if the recombinational events were reciprocal, a band that corresponds to a gene containing both the +25 and Δ23 deletions would be seen.

DNA from several TK^+ cell lines was digested with restriction endonucleases. First, cellular DNA was digested with a combination of Hind III, Bam HI, and Kpn I (referred to as HBK). Cleavage of −109 DNA yielded 750- and 960-bp fragments; +25 DNA gave the same 960-bp 3′ fragment and a shorter 610-bp 5′ fragment; and Δ23 gave a single 1710-bp fragment spanning the entire region between the Bam HI and Hind III sites (Fig. 1C).

DNA of a TK^+ cell line generated by a mixture of +25 and Δ23 should have 960- and 610-bp fragments from +25 and a 1710-bp fragment from Δ23. If recombination occurred to generate a functional TK gene, then a 750-bp fragment, corresponding to the 5′ end of the wild-type gene also should be present. If the reciprocal recombination event occurred, a 1525-bp fragment, representative of a double-deletion mutant gene might be present. The results of the Southern blot are shown in Fig. 1A. The diagnostic 750-bp band was visualized in each of five cell lines examined. The 1525-bp band was visualized in four of the five cell lines. These data indicate that recombination occurred to generate both functional and double-deletion genes.

Cellular DNA's were digested with both Eco RI and Kpn I to confirm these findings. Cleavage of −109 DNA yielded 720- and 990-bp fragments; the +25 deletion removed the 5′ Eco RI site and therefore generated a 990-bp TK fragment and a 4600-bp TK-pBR322 fragment; and Δ23 yielded a 1710-bp fragment.

Table 1. Transfer frequency of TK deletion mutants alone and after coprecipitation. Circular plasmid DNA (3 μg per dish) was coprecipitated with calcium phosphate as described (*20*) onto 10^6 Ltk^- cells. Hypoxanthine-aminopterin-thymidine (*21*) selection was added 24 to 36 hours later, and colonies were counted after 2 weeks. Plasmids are shown in Fig. 1. A wild-type gene, −109, was used as a positive control; +25 contains a deletion of 5′ control sequences; and Δ23 contains a deletion within the structural gene. An increase in frequency of colonies when +25 and Δ23 were mixed suggests that recombination between the two deletions to generate a functional TK gene occurred.

Plasmid DNA	Number of colonies/number of petri dishes					Total	Frequency per dish
	1	2	3	4	5		
−109	4/2	15/5	81/4	67/4	58/4	225/19	11.8
+25	0/4	0/5	0/5	1/4	2/5	3/23	0.13
Δ23	0/4	0/5	0/5	0/4	0/4	0/23	0.0
Mixture of +25 and Δ23*	3/10	3/5	10/5	10/5	13/10	44/35	1.3

*1.5 μg of each plasmid.

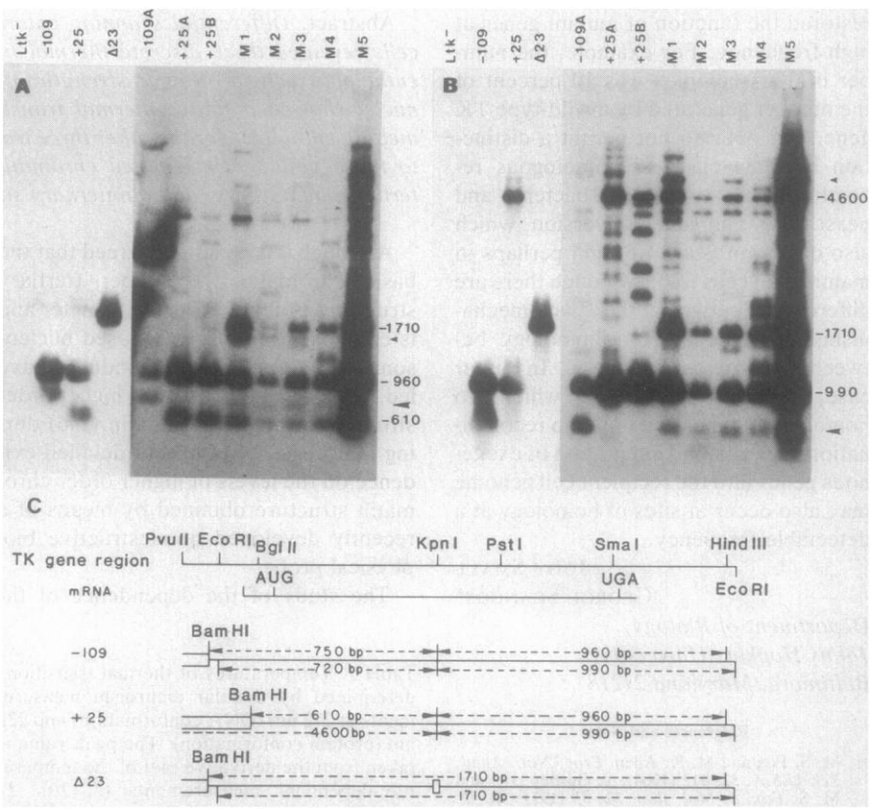

Fig. 1. (A and B) Southern blots of cellular DNA from TK^+ cell lines. DNA (10 μg from each cell line) was digested with 80 units of Kpn I for 16 hours, then with 40 units each of Hind III and Bam HI (A) or 40 units of Eco RI (B) for 16 hours. DNA fragments were separated on 1.2 percent agarose gels and transferred to nitrocellulose (*17*). Hybridization to ^{32}P-labeled 2.8-kbp Bam HI–Bgl II TK fragment of pTKxl was as described (*22*). Lanes −109, +25, and Δ23 contain 10 μg of Ltk^- cellular DNA mixed with 50 pg of the respective plasmid; −109A is a control cell line generated by wild-type −109; +25A and +25B were generated by +25 alone; and the remaining lanes, M1 through M5, resulted from mixtures of +25 and Δ23. (A) The 1700-, 960-, and 610-bp fragments are derived from plasmids +25 and Δ23. The large arrowhead points to the 750-bp recombinant fragment. The small arrowhead indicates the 1575-bp fragment generated by a double-deletion recombinant. (B) The 4600-, 1700-, and 990-bp fragments refer to parental fragments from +25 or Δ23. The large arrowhead points to the 720-bp recombination-generated fragment, and the small arrowhead points to the 5590-bp double-deletion recombinant fragment. (C) Partial restriction maps of plasmids −109, +25, and Δ23. The partial restriction enzyme map, the transcription map, and locations of deletions are from (*16*). The precise end points of the deletion of Δ23 encompassing the Kpn I site have not been defined. Restriction analyses show that the Kpn I site is absent, and the Pst I and Bgl II sites are present. The mobility of the Bgl II–Pst I fragment on 1 percent agarose gels is indistinguishable from that of the same fragment in −109, indicating that the deletion is small. Each gene has a Bam HI linker on the 5′ end and a Hind III site on the 3′ end, and each was cloned into the Bam HI and Hind III sites of pBR322. The TK gene region from which all of the plasmids were derived is shown, along with the TK mRNA. For each plasmid, the TK gene is indicated by the solid line, and the deletion in each case is indicated by the double line. The dotted lines above each gene indicate fragments generated by Hind III, Bam HI, and Kpn I digestion, and the dotted lines below the gene represent Eco RI–Kpn I fragments.

ment (Fig. 1C). If +25 and Δ23 recombined to yield a functional TK gene, a recombinant 720-bp fragment representing the 5′ end of a functional gene should be generated. In this instance, a double-deletion gene formed by the reciprocal recombination event should generate a 5590-bp band (Fig. 1B). In the lanes that have DNA from cell lines generated by mixtures of +25 and Δ23, the 720-bp fragment representative of recombination is present. The 5590-bp fragment is visualized in three of the five cell lines.

These data indicate that recombination between homologous genes occurred during DNA-mediated gene transfer and that the recombination events restored the function of mutant genes at high frequency. For example, the number of TK^+ colonies was 10 percent of the number generated by a wild-type TK gene. Our data do not permit a distinction between classical homologous recombination, as seen in bacteria and yeast (*1–4*), and gene conversion, which also occurs in yeast (*18*) and perhaps in mammalian cells (*19*). Although there are differences between the two mechanisms, both depend on homology between two regions of DNA. In either case, the high frequency with which two homologous genes can undergo recombination suggests that integration of exogenous genes into the recipient cell genome may also occur at sites of homology at a detectable frequency.

JUDY SMALL
GEORGE SCANGOS*

Department of Biology,
Johns Hopkins University,
Baltimore, Maryland 21218

References and Notes

1. M. S. Fox and M. K. Allen, *Proc. Natl. Acad. Sci. U.S.A.* **52**, 412 (1964); T. Gurney, Jr., and M. S. Fox, *J. Mol. Biol.* **32**, 83 (1971); R. D. Hotchkiss and M. Gabor, *Annu. Rev. Genetics* **4**, 193 (1970).
2. D. T. Stinchcomb, K. Struhl, R. W. Davis, *Nature (London)* **282**, 39 (1979).
3. K. Struhl, D. T. Stinchcomb, S. Scherer, R. W. Davis, *Proc. Natl. Acad. Sci. U.S.A.* **76**, 1035 (1979).
4. A. Hinnen, J. B. Hicks, G. R. Fink, *ibid.* **75**, 1929 (1978).
5. A. Pellicer, M. Wigler, R. Axel, S. Silverstein, *Cell* **14**, 133 (1978).
6. M. Wigler, A. Pellicer, S. Silverstein, R. Axel, *ibid.*, p. 725.
7. A. Pellicer *et al.*, *Science* **209**, 1414 (1980).
8. G. Scangos, K. M. Huttner, D. K. Juricek, F. H. Ruddle, *Mol. Cell. Biol.* **1**, 111 (1981).
9. G. Scangos and F. H. Ruddle, *Gene* **14**, 1 (1981).
10. R. Holliday, *Symp. Soc. Gen. Microbiol.* **20**, 359 (1970).
11. H. Gruneberg, *Genet. Res.* **7**, 58 (1962).
12. S. A. Latt, *Proc. Natl. Acad. Sci. U.S.A.* **71**, 3162 (1974).
13. C. Brack, M. Hirama, R. Lenhard-Schuller, S. Tonegawa, *Cell* **15**, 1 (1978).
14. D. A. Jackson, in *Introduction of Macromolecules into Viable Mammalian Cells*, R. Baserga, C. Croce, G. Rovera, Eds. (Liss, New York, 1980), p. 65; C. T. Wake and J. H. Wilson. *Proc. Natl. Acad. Sci. U.S.A.* **76**, 2876 (1979); P. Upcroft, B. Carter, C. Kidson, *Nucleic Acids Res.* **8**, 5835 (1980).
15. P. J. Kretschmer, A. H. Bowman, M. H. Huberman, L. Sanders-Haigh, L. Killos, W. F. Anderson, *Nucleic Acids Res.* **9**, 6199 (1981); R. A. Anderson, T. Krakauer, R. D. Camerini-Otero. *Proc. Natl. Acad. Sci. U.S.A.* **79**, 2748 (1982).
16. S. L. McKnight, E. R. Gavis, R. Kingsbury, R. Axel, *Cell* **25**, 385 (1981).
17. E. Southern, *J. Mol. Biol.* **98**, 503 (1975).
18. S. Fogel and R. Mortimer, *Proc. Natl. Acad. Sci. U.S.A.* **62**, 96 (1969).
19. J. M. Roberts and R. Axel, *Cell* **29**, 109 (1982).
20. K. M. Huttner, J. A. Barbosa, G. Scangos, D. Prautcheva, F. H. Ruddle, *J. Cell Biol.* **91**, 153 (1981).
21. E. H. Szybalska and W. Szybalski, *Proc. Natl. Acad. Sci. U.S.A.* **48**, 2026 (1962); J. W. Littlefield, *Science* **145**, 709 (1964).
22. B. Christy and G. Scangos, *Proc. Natl. Acad. Sci. U.S.A.* **79**, 6299 (1982).
23. We thank S. L. McKnight for the −109 and +25 plasmids, E. Fyrberg and D. Powers for critical evaluation of the manuscript, G. Ketner for helpful suggestions, and D. Warr for manuscript preparation. This work was supported by NSF award PCM8105296. J.S. was supported by NIH predoctoral training grant GM 5T32 GM07231-08. This is contribution number 1187 from the Department of Biology.
* To whom all correspondence should be addressed.

13 September 1982; revised 28 October 1982

Quaternary and Quinternary Structures of Native Chromatin DNA in Liver Nuclei: Differential Scanning Calorimetry

Abstract. *Differential scanning calorimetry of chromatin isolated from rat liver cells revealed three discrete thermal transitions whose temperatures and melting enthalpies depend on ionic strength in the range 0 to 600 millimolar NaCl. Intact nuclei showed a fourth thermal transition at a lower temperature and different melting enthalpies for the other three transitions still present at temperatures similar to those obtained in isolated chromatin. The data are discussed in terms of the tertiary, quaternary, and quinternary structures of chromatin DNA.*

Although it is generally agreed that the basic chromatin DNA fiber (tertiary structure) is about 110 Å in diameter and is composed of closely apposed nucleosomes (*1*), experimental findings have led to several models for the higher order structure in native chromatin (*2–6*) during interphase. We present detailed evidence on the levels of higher order chromatin structure obtained by means of a recently developed nondestructive biophysical probe.

The study of the dependence of the optical properties of biological macromolecules on temperature is a current method of identifying their discrete conformational states, and it provides indirect information on the thermodynamics of the transitions (*6–8*). However, this approach has serious limitations (*6–8*).

Using a sensitive differential scanning calorimeter (Perkin-Elmer, DSC II), we have begun a systematic study of enthalpy changes versus temperature for both chromatin and intact nuclei in a range of ionic strengths far greater than the 7 m*M* limit possible with traditional spectrophotometry or spectropolarimetry. Thermal profiles of nuclei had up to now been prohibitive not only because of their relatively high physiological strength, but also because of their high sedimentation and light scattering. With calorimetry, it is possible to study the stability of the DNA and its higher order structures "in situ."

Figure 1 shows the heat capacity (dq/dT) versus temperature, in the range 300 to 400 K, for isolated chromatin in 1 m*M* tris-HCl, *p*H 8, at 0, 10, 50, and 600 m*M* NaCl. Three transitions (I, II, and III), whose temperature values change slightly with salt concentration, are clearly and reproducibly identifiable. As shown in Fig. 1 and summarized in Fig. 2, the enthalpy change (ΔH) for isolated chromatin varies with salt concentration; the enthalpy change decreases between 0 and 10 m*M* and then remains constant for transition I, increases steadily for transition III, and increases sharply up to 50 m*M* and then decreases sharply at 600 m*M* for transition II.

Table 1. Temperatures of thermal transitions determined by circular dichroism measurements at 272 nm (DNA conformation) and 223 nm (protein conformation). The peak value is taken from the derivative plot of the temperature-dependent measurements (*7, 10*). T_S (negative derivative) and T_M (positive derivative) represent, respectively, the superhelix-helix and helix-coil transitions as determined by the molar ellipticity at 272 nm. T_P represents the position of the only peak in the derivative plot of the molar ellipticity at 223 nm. Ellipticity and absorbancy, at given wavelength, were measured on our modified J-40 spectropolarimeter equipped with both circulatory bath and PG-VL thermostat (*8*). At 1 to 7 m*M* tris-HCl, an abrupt decrease in molar ellipticity could be monitored at 272 nm, even if the thermal transition was not completed by 367 K; at higher ionic strengths, this decrease was not apparent.

Sample	Temperature (°K)		
	T_M	T_S	T_P
Protein-free DNA at 1 m*M* tris	~ 333		
Protein-free DNA at 50 m*M* NaCl	~ 355		
Chromatin at 1 m*M* tris	> 367	~ 360	~ 345